Dye-sensitized solar cells: investigation of D-A-π-A organic sensitizers based on [1,2,5]selenadiazolo[3,4-*c*]pyridine

Ekaterina A. Knyazeva[a,b], Wenjun Wu[c, e, *], Timofey N. Chmovzh,[a] Neil Robertson[c,*], J. Derek Woollins[d], Oleg A. Rakitin[a,b,*]

[a]*N. D. Zelinsky Institute of Organic Chemistry, Russian Academy of Sciences, 119991 Moscow, Russia*

[b]*Nanotechnology Education and Research Center, South Ural State University, 454080 Chelyabinsk, Russia*

[c]*EaStCHEM School of Chemistry, University of Edinburgh, Edinburgh EH9 3FJ, UK*

[d]*EaStCHEM School of Chemistry, University of St. Andrews, St. Andrews, Fife KY16 9ST, UK*

[e]*Key Laboratory for Advanced Materials and Institute of Fine Chemicals, East China University of Science & Technology, Shanghai 200237, China.*

Abstract

We report two series of D-A-π-A metal-free organic sensitizers for dye-sensitized solar cells (DSSCs) based on triphenylamine and N-hexyl-carbazole as electronic donors, respectively. Through varying auxiliary acceptors and π-spacers, several significant consequences on cell efficiency were identified: i) a broadened UV-Vis absorption spectrum and low-lying LUMO level with [1,2,5]selenadiazolo [3,4-c] pyridine as auxiliary acceptor; ii) compensation for the absorption valley around 400nm in the UV-vis spectra by the introduction of a thiophene unit into the π-bridge; iii) effective improvement of the power conversion efficiency (PCE) by means of cosensitization, leading to dye **OKT-1**, 3.10% PCE, increased to 4.19% with squaraine dye **SQ2** as co-sensitizer. The design criteria identified have opened the door for further optimization of this new dye family.

Corresponding author. Tel.: +7-499-135-53-27; fax: +7-499-135-53-28; e-mail: orakitin@ioc.ac.ru; wjwu@ecust.edu.cn; neil.robertson@ed.ac.uk.

1. Introduction

The dye-sensitized solar cell (DSSC) is one of the most promising photovoltaic technologies, and has attracted much attention not only at science but also at industry level as the third generation solar cell technology closest to commercialization due to its potential for low-cost

electricity production as well as its potential as a portable energy supply [1,2]. In DSSCs, sunlight is absorbed by molecular dyes that are attached onto the surface of a wide band gap semiconducting oxide (typically TiO_2). The dye molecules act as sensitizers, and inject electrons into the conduction band of metal oxide upon photoexcitation [3]. The injected electrons are conducted through the nanostructured metal oxide to reach the external circuit, and the oxidized dyes are regenerated by a redox couple present in the electrolyte. The dye is one of the most important components of the solar cell since it can be engineered to increase the power conversion efficiency. Organic dyes are very attractive molecules due to their low cost, ease of structure tuning and high molar extinction coefficients. High-performance organic sensitizers usually feature a donor-π-bridge-acceptor (D−π−A) structure [2, 4]. The electronic interaction between donor (D) and acceptor (A) results in strong charge-transfer absorption bands that harvest sunlight for photon-to-electron conversion. In 2011, Zhu et al. proposed a concept of a D−A−π−A motif for designing a new generation of efficient and stable organic sensitizers, incorporating into the π-bridge an additional auxiliary acceptor to tailor molecular structures and optimize energy levels [5]. Several kinds of electron-withdrawing units (such as benzothiadiazole, benzotriazole, quinoxaline, phthalimide, diketo-pyrrolopyrrole and others) have been systematically exploited for viable D−A−π−A structures and demonstrates a significant increase in the photovoltaic efficiency and a significant improvement in the stability of organic sensitizers as well as devices [6-8].

The novel [1,2,5]selenadiazolo[3,4-*c*]pyridine moiety has previously been used in low band gap polymers which exhibited highly red-shifted absorption maxima from those of the benzothiadiazole analogues [9,10]. In this work we therefore aimed to explore new organic dyes based on the [1,2,5]selenadiazolo[3,4-*c*]pyridine unit concept and to obtain π-conjugated condensed-polycyclic structures. We introduced not only triphenylamine but also carbazole building blocks with the [1,2,5]selenadiazolo[3,4-*c*]pyridine unit (Scheme 1). Herein, the first few dyes using this new internal acceptor were synthesized, characterized and tested. The photo-physical and photo-electric properties of these dyes were systemically studied to identify useful design criteria for the discovery of further new dyes within this family. We determined the photovoltaic performance for four dyes which showed the most appropriate energy-level match, and understanding their photophysical, orbital and photoelectric conversion characteristics will enable further design of new sensitizers, in particular the bathochromic shift in UV-visible absorption spectrum and LUMO energy level tuning with selenium in place of sulfur. In addition, via cosensitization with the squaraine-derived dye

SQ2, possessing effective absorption in the near infrared region, the photoelectrical conversion efficiency (PCE) of **OKT-1** was significantly increased 35% from 3.10% to 4.19% through expanding the sensitizer spectral response.

2. Experimental details

2.1. Materials and reagents

The reagents were purchased from commercial sources and used as received. 4,7-dibromo-[1,2,5]thiadiazolo[3,4-*c*]pyridine (**1**) [11], (4-(diphenylamino)phenyl)boronic acid (**3**) [12], (9-hexyl-9*H*-carbazol-3-yl)boronic acid (**4**) [13], *tert*-butyl 2-cyano-3-(4-(4,4,5,5-tetramethyl-1,3,2-dioxaborolan-2-yl)phenyl)acrylate (**5**) [14] and *tert*-butyl 2-cyano-3-(5-(4,4,5,5-tetramethyl-1,3,2-dioxaborolan-2-yl)thiophen-2-yl)acrylate (**6**) [14] were prepared according to the published methods and characterized by NMR spectra. The synthetic routes for these building blocks are shown in Scheme 2. All synthetic operations were performed under a dry argon atmosphere. Solvents were purified by distillation from the appropriate drying agents.

2.2. Analytical instruments

Elemental analyses were performed on Perkin Elmer 2400 Elemental Analyser. Melting points were determined on a Kofler hot-stage apparatus and are uncorrected. ^{1}H and ^{13}C NMR spectra were taken with a Bruker AM-300 machine (at frequencies of 300.1 and 75.5 MHz, respectively) in $CDCl_3$ solutions, with TMS as the standard. *J* values are given in Hz. MS spectra (EI, 70 eV) were obtained with a Finnigan MAT INCOS 50 instrument. High-resolution MS spectra were measured on a Bruker micrOTOF II instrument using electrospray ionization (ESI). The measurement was operated in a positive ion mode (interface capillary voltage –4500 V) or in a negative ion mode (3200 V); mass range was from m/z 50 to m/z 3000 Da; external or internal calibration was done with Electrospray Calibrant Solution (Fluka). A syringe injection was used for solutions in acetonitrile, methanol, or water (flow rate 3 $\mu L.min^{-1}$). Nitrogen was applied as a dry gas; interface temperature was set at 180°C. IR spectra were measured with a Specord M-80 instrument in KBr pellets.

2.3. General procedure for fabrication and characterization of DSSCs

Titanium dioxide paste 18NR-T and 18NR-AO (Dyesol) were deposited onto clean fluorine doped tin oxide conductive glass (FTO, 3 mm thick, 8 Ω sheet resistance, Solaronix) by screen printing and the film thickness was approx. 12 μm (8 μm 18NR-T

adsorbed layer plus 4 μm 18NR-AO scattering layer). The TiO_2 electrodes (area = 0.28 cm^2) were gradually heated on hot plate with programmed temperature at 325 °C for 5 °C min, 375 °C for 5 min, 450 °C for 15 min and 500 °C for 15 min, cooled to room temperature, treated with a dilute solution of $TiCl_4$ (40 mM, 75 °C for 30 mins) and sintered at 500 °C for 30 min. The electrodes were allowed to cool (80-100 °C) and immersed into a dimethylformamide (DMF) and dichloromethane (DCM) (V:V=7:3) solution of **OKT**s (3 mM) overnight. For the cosensitization, a step-by-step method was employed with dipping time of 15h for **OKT-1** and 5h for **SQ2** in acetonitrile and 1-butanol (V:V=85:15) solution with 6 mM chenodeoxycholic acid (CDCA), respectively. Then, the electrodes were removed and washed with ethanol and dried. Counter electrodes were platinized using Platisol T/SP (Solaronix, Swiss) by doctor-blading and heated to 400 °C for 15 minutes. The solar cells were assembled by sandwiching the two electrodes together using a sealant (Bynel, 25 μm), and heated to 120 °C, applying even pressure to ensure the Bynel melted evenly. Electrolyte was vacuum filled into the hole and the hole was sealed by Bynel and a cover glass. The electrolyte used was 0.03 M iodine (I_2), 0.01 M guanidinium thiocyanate (GuNCS), 0.5 M *tert*-butylpyridine (TBP), 0.6 M 1-butyl-3-methyl-imidazolium iodide (BMII) in acetonitrile:valeronitrile (MeCN:VN) 85:15.

The current-voltage (I-V) curves were measured (Potentiostat/Galvanostat, Metrohm Autolab B.V.) under simulated AM 1.5 sunlight at 100 mW cm^{-2} irradiance generated by a Class AAA small collimated Beam Solar simulator (SF300A, Sciencetech Inc.), with the intensity calibrated by Si reference cell. The mismatch factor between the simulated sunlight and the actual solar spectrum is not corrected. The solar cells were masked with a metal aperture to define the active area, typically 0.1256 cm^2.

2.4. The detailed experimental procedures and characterization data

2.4.1 Optical characterization

Solution UV-Visible absorption spectra were recorded using a Jasco V-670 UV/Vis/NIR spectrophotometer controlled with SpectraManager software. All samples were measured in a 1 cm cell at room temperature with 4×10^{-5} mol mL^{-1} concentration in DMF and DCM (V:V=7:3).

2.4.2 Electrochemical Characterization

All cyclic voltammetry measurements were carried out in freshly distilled DMF and DCM (V:V=7:3) using 0.1 M $TBAPF_6$ electrolyte in a three electrode system, with each solution being purged with N_2 prior to measurement. The working electrode was a Pt disk. The

reference electrode was Ag/AgCl and the counter electrode was a Pt rod. All measurements were made at room temperature using a mAUTOLAB Type III potentiostat, driven by the electrochemical software GPES. Cyclic voltammetry (CV) measurements used scan rates of 0.1 V s^{-1}.

2.5 Synthesis and characterization of compounds:

2.5.1 4,7-Dibromo-[1,2,5]selenadiazolo[3,4-c]pyridine (2)

A mixture of 3,4-diamino-2,5-dibromopyridine (532 mg, 2.0 mmol) and SeO_2 (244 mg, 2.2 mmol) in EtOH (8.0 ml) was refluxed for 10 min and cooled. Precipitate was filtered, washed with EtOH and dried. Yield 573 mg (84%). IR and NMR spectra are similar to the literature data [9].

*2.5.2 General procedure for the cross-coupling reactions of [1,2,5]chalcogenadiazolo[3,4-c]pyridines **1**, **2** and arylboronic acids **3**, **4***

The mixture of 4,7-dibromo-[1,2,5]chalcogenadiazolo[3,4-*c*]pyridine **1**, **2** (1.0 mmol), (het)arylboronic acid **3**, **4** (1.1 mmol), solution of 2M K_2CO_3 (4 ml) and $Pd(PPh_3)_4$ (3 mol %) in THF (10 ml) was degassed by argon and refluxed under argon for 20 h. On completion, the mixture was poured into water and extracted with DCM (3 × 50 ml). The combined organic phases were washed with brine (2 × 50 ml), dried over $MgSO_4$, filtered, and concentrated under reduced pressure.

4-(7-Bromo-[1,2,5]thiadiazolo[3,4-c]pyridin-4-yl)-N,N-diphenylaniline (***7a***)

The crude product was purified by column chromatography using DCM:hexane (2:1) as the eluent to afford **7a** as a dark red solid (82%); IR and NMR spectra are similar to the literature data [15].

4-(7-Bromo-[1,2,5]selenadiazolo[3,4-c]pyridin-4-yl)-N,N-diphenylaniline (***7b***)

The crude product was purified by column chromatography using DCM:hexane (2:1) as the eluent to afford **7b** as a violet solid (72%); ^{1}H NMR (300 MHz, $CDCl_3$): δ 7.07-7.35 (m, 12H), 8.42 (d, ^3J = 11.0 Hz, 2H), 8.62 (s, 1H); ^{13}C NMR (100 MHz, $CDCl_3$): δ 121.3, 124.4, 125.8, 129.6, 131.8, 146.9 (6 C-H), 111.1, 129.2, 145.0, 150.6, 153.7, 155.1, 160.5; ^{77}Se NMR (75 MHz, $CDCl_3$): δ 1471.2; ESI-MS, *m/z*: found 506.9708; calc. for $C_{23}H_{15}BrN_4Se$ $[M+H]^+$ 506.9716; IR, ν, cm^{-1}: 3058, 3035, 2920, 1588, 1535, 1489, 1327, 1274, 1193, 754, 696.

7-Bromo-4-(9-hexyl-9H-carbazol-3-yl)-[1,2,5]thiadiazolo[3,4-c]pyridine (***7c***)

The crude product was purified by column chromatography using DCM:hexane (2:1) as the eluent to afford **7c** as an orange solid (80%); ^{1}H NMR (300 MHz, $CDCl_3$): δ 0.81-0.98

(m, 3H), 1.26-1.53 (m, 6H), 1.91-1.98 (m, 2H), 4.38 (t, ^3J = 7.2 Hz, 2H), 7.32 (dd, ^3J = 8.7 Hz, ^3J = 5.9 Hz, 1H), 7.46-7.58 (m, 3H), 8.26 (d, ^3J = 7.7 Hz, 1H), 8.80 (dd, ^3J = 8.8, ^4J = 1.8 Hz, 1H), 8.83 (s, 1H), 9.46 (d, ^4J = 1.4 Hz, 1H); ^{13}C NMR (100 MHz, $CDCl_3$): δ 14.0, 22.5, 27.0, 29.0, 31.6, 43.3, 107.9, 108.8, 109.1, 119.7, 120.8, 123.0, 123.3, 123.7, 126.2, 126.9, 127.7, 141.0, 142.1, 145.7, 149.5, 153.1, 156.7; ESI-MS, *m/z*: found 465.0731; calc. for $C_{23}H_{21}BrN_4S$ $[M+H]^+$ 465.0743; IR, ν, cm^{-1}: 2928, 2852, 1596, 1469, 1444, 1361, 1326, 1265, 1119, 744, 727, 560.

7-Bromo-4-(9-hexyl-9H-carbazol-3-yl)-[1,2,5]selenadiazolo[3,4-c]pyridine (***7d***)

The crude product was purified by column chromatography using DCM:hexane (2:1) as the eluent to afford **7d** as a dark red solid (94%); ^{1}H NMR (300 MHz, $CDCl_3$): δ 0.87-0.92 (m, 3H), 1.28-1.44 (m, 6H), 1.81-1.97 (m, 2H), 4.35 (t, ^3J = 7.2 Hz, 2H), 7.32 (dd, ^3J = 8.7 Hz, ^3J = 5.9 Hz, 1H), 7.44-7.54 (m, 3H), 8.23 (d, ^3J = 7.7 Hz, 1H), 8.65 (br s, 1H), 8.67 (s, 1H), 9.34 (d, ^4J = 1.4 Hz, 1H); ^{13}C NMR (100 MHz, $CDCl_3$): δ 14.0, 22.6, 27.0, 29.0, 31.6, 43.4, 108.8, 109.1, 110.9, 119.7, 120.8, 123.3, 123.4, 123.7, 126.2, 127.6, 128.3, 141.1, 142.1, 145.2, 155.0, 155.3, 160.5; ESI-MS, *m/z*: found 513.0185; calc. for $C_{23}H_{21}BrN_4Se$ $[M+H]^+$ 513.0186; IR, ν, cm^{-1}: 2924, 2852, 1596, 1442, 1364, 1330, 1255, 1116, 908, 790, 745, 534.

*2.5.3 General procedure for the of cross-coupling reaction of mono-adducts **7a-d** and esters of (het)arylboronic acids **5, 6***

The mixture of mono-adduct **7a-d** (0.25 mmol), ether of (het)arylboronic acid **5**, **6** (0.3 mmol), solution of 2M K_2CO_3 (1 ml) and $Pd(PPh_3)_4$ (3 mol %) in mixture of THF (5 ml) and toluene (5 ml) was degassed by argon and refluxed under argon for 10 h. After cooling additional amount of ether of boronic acid (0.3 mmol) and $Pd(PPh_3)_4$ (3 mol %) were added and the reaction mixture was refluxing for 10 h. On completion, the mixture was poured into water and extracted with DCM (3 × 50 ml). The combining organic phases were washed with brine (2 × 50 ml), dried over $MgSO_4$, filtered, and concentrated under reduced pressure.

tert-Butyl 2-cyano-3-(4-(4-(4-(diphenylamino)phenyl)-[1,2,5]thiadiazolo[3,4-c]pyridin-7-yl)phenyl)acrylate (***8a***)

The crude product was purified by column chromatography using DCM:ethyl acetate (10:1) as the eluent to afford **8a** as a dark red solid (81%); ^{1}H NMR (300 MHz, $CDCl_3$): δ 1.62 (s, 9H), 7.09-7.18 (m, 2H), 7.19-7.39 (m, 10H), 8.17 (d, ^3J = 8.8 Hz, 2H), 8.22 (d, ^3J = 8.8 Hz, 2H), 8.25 (s, 1H), 8.60 (d, ^3J = 8.8 Hz, 2H), 8.86 (s, 1H); ^{13}C NMR (100 MHz, $CDCl_3$): δ 27.9, 83.9, 104.9, 115.7, 121.1, 124.3, 125.7, 129.52, 129.56, 129.7, 131.3, 131.4,

131.6, 133.7, 135.3, 139.0, 146.7, 149.6, 153.0, 153.8, 156.6, 161.1, 161.2; ESI-MS, *m/z*: found 608.2054; calc. for $C_{37}H_{29}N_5O_2S$ $[M+H]^+$ 608.2100; IR, ν, cm^{-1}: 2978, 2920, 2852, 2221, 1721, 1590, 1490, 1450, 1368, 1318, 1284, 1155, 1090, 838, 756, 697, 513.

tert-Butyl 2-cyano-3-(4-(4-(4-(diphenylamino)phenyl)-[1,2,5]selenadiazolo[3,4-c]pyridin-7-yl)phenyl)acrylate (***8b***)

The crude product was purified by column chromatography using DCM:ethyl acetate (10:1) as the eluent to afford **8b** as a violet solid (82%); ^{1}H NMR (300 MHz, $CDCl_3$): δ 1.63 (s, 9H), 7.11-7.16 (m, 2H), 7.19-7.24 (m, 6H), 7.31-7.36 (m, 4H), 8.13 (d, ^3J = 8.8 Hz, 2H), 8.17 (d, ^3J = 8.8 Hz, 2H), 8.25 (s, 1H), 8.49 (d, ^3J = 8.6 Hz, 2H), 8.65 (s, 1H); ^{13}C NMR (100 MHz, $CDCl_3$): δ 27.9, 83.9, 104.8, 115.5, 120.9, 124.5, 125.8, 129.6, 129.8, 129.9, 131.2, 131.6, 132.1, 133.8, 135.3, 139.4, 146.5, 150.8, 153.1, 153.9, 155.2, 161.1, 161.8; ^{77}Se NMR (75 MHz, $CDCl_3$): δ 1507.9; ESI-MS, *m/z*: found 656.1534; calc. for $C_{37}H_{29}N_5O_2Se$ $[M+H]^+$ 656.1534; IR, ν, cm^{-1}: 2978, 2928, 2854, 2221, 1716, 1589, 1487, 1449, 1370, 1330, 1284, 1156, 842, 758, 698.

tert-Butyl 2-cyano-3-(5-(4-(4-(diphenylamino)phenyl)-[1,2,5]selenadiazolo[3,4-c]pyridin-7-yl)thiophen-2-yl)acrylate (***8c***)

The crude product was purified by column chromatography using DCM:ethyl acetate (10:1) as the eluent to afford **8c** as a violet solid (96%); ^{1}H NMR (300 MHz, $CDCl_3$): δ 1.26 (s, 9H), 7.14-7.38 (m, 12H), 7.91 (d, ^3J = 4.1 Hz, 1H), 8.09 (d, ^3J = 4.1 Hz, 1H), 8.27 (s, 1H), 8.55 (d, ^3J = 8.6 Hz, 2H), 8.90 (s, 1H); ^{13}C NMR (100 MHz, $CDCl_3$): δ 29.0, 83.5, 116.2, 120.2, 120.3, 121.0, 124.4, 125.8, 127.9, 129.3, 129.6 132.0, 136.9, 137.2, 141.8, 145.2, 146.7, 150.8, 151.8, 155.0, 157.0, 159.5, 161.7; ESI-MS, *m/z*: found 662.1112; calc. for $C_{35}H_{27}N_5O_2SSe$ $[M+H]^+$ 662.1125; IR, ν, cm^{-1}: 2957, 2925, 2854, 2215, 1738, 1710 1585, 1489, 1432, 1329, 1270, 1153.

tert-Butyl 2-cyano-3-(4-(4-(9-hexyl-9H-carbazol-3-yl)-[1,2,5]thiadiazolo[3,4-c]pyridin-7-yl)phenyl)acrylate (***8d***)

The crude product was purified by column chromatography using DCM:ethyl acetate (10:1) as the eluent to afford **8d** as a dark red solid (96%); ^{1}H NMR (300 MHz, $CDCl_3$): δ 0.90 (t, ^3J =6.9 Hz, 3H), 1.27-1.51 (m, 6H), 1.65 (s, 9H), 1.85-2.00 (m, 2H), 4.34 (t, ^3J = 7.2 Hz, 2H), 7.31 (dd, ^3J = 8.7 Hz, ^3J =5.9 Hz, 1H), 7.42-7.58 (m, 3H), 8.12-8.21(m, 4H), 8.23 (s, 1H), 8.26 (d, ^3J = 7.7 Hz, 1H), 8.80 (dd, ^3J =8.8 Hz, ^4J = 1.6 Hz, 1H), 8.88 (s, 1H), 9.50 (d, ^4J = 1.4 Hz, 1H); ^{13}C NMR (100 MHz, $CDCl_3$): δ 14.0, 22.5, 26.9, 28.0, 28.9, 31.5, 43.3, 83.8, 104.6, 108.7, 109.0, 115.8, 119.6, 120.8, 123.1, 123.32, 123.39, 123.9, 126.1, 127.5, 127.9,

129.4, 131.33, 131.38, 139.3, 141.0, 142.1, 143.2, 149.8, 153.0, 153.9, 156.5, 161.3; ESI-MS, *m/z*: found 614.2573; calc. for $C_{37}H_{35}N_5O_2S$ $[M+H]^+$ 614.2584; IR, ν, cm^{-1}: 2929, 2857, 2220, 1718, 1593, 1445, 1285, 1156, 838, 747, 520.

tert-Butyl 2-cyano-3-(4-(4-(9-hexyl-9H-carbazol-3-yl)-[1,2,5]selenadiazolo[3,4-c]pyridin-7-yl)phenyl)acrylate (***8e***)

The crude product was purified by column chromatography using DCM:ethyl acetate (10:1) as the eluent to afford **8d** as a dark red solid (91%); ^{1}H NMR (300 MHz, $CDCl_3$): δ 0.6 (t, ^3J =7.1 Hz, 3H), 1.18-1.40 (m, 6H), 1.57 (s, 9H), 2.48-2.52 (m, 2H), 4.43 (t, ^3J = 7.1 Hz, 2H),7.27 (dd, ^3J = 8.2 Hz, ^3J = 6.8 Hz, 1H), 7.51 (dd, ^3J = 8.8 Hz, ^3J = 6.8 Hz, 1H), 7.64 (d, ^3J = 8.2 Hz, 1H), 7.73 (d, ^3J = 8.8 Hz, 1H), 8.13-8.29 (m, 5H), 8.35 (br s, 1H), 8.75 (s, 1H), 8.77 (d, ^3J =1.4 Hz, 1H) 9.43(d, ^4J = 1.4 Hz, 1H); ^{13}C NMR (100 MHz, $CDCl_3$): δ 13.4, 21.6, 25.8, 27.4, 28.2, 30.6, 42.9, 83.1, 103.8, 108.7, 109.4, 115.4, 119.2, 120.0, 122.0, 122.3, 122.8, 125.1, 125.8, 127.9, 128.1, 129.6, 130.4, 130.7, 139.6, 140.5, 141.2, 142.0, 153.3, 154.2, 154.5, 159.7, 160.5; ^{77}Se NMR (75 MHz, $CDCl_3$): δ 1560.4; ESI-MS, *m/z*: found 662.2016; calc. for $C_{37}H_{35}N_5O_2Se$ $[M+H]^+$ 662.2032; IR, ν, cm^{-1}: 2929, 2859, 2224, 1722, 1596, 1439, 1368, 1288, 1143, 1027, 754.

tert-Butyl 2-cyano-3-(5-(4-(9-hexyl-9H-carbazol-3-yl)-[1,2,5]thiadiazolo[3,4-c]pyridin-7-yl)thiophen-2-yl)acrylate (***8f***)

The crude product was purified by column chromatography using DCM:ethyl acetate (10:1) as the eluent to afford **8f** as a dark red solid (92%); ^{1}H NMR (300 MHz, $CDCl_3$): δ 0.80-0.95 (m, 3H), 1.19-1.46 (m, 6H), 1.62 (s, 9H), 1.78-1.94 (m, 2H), 4.22 (t, ^3J = 7.0 Hz, 2H), 7.14-7.52 (m, 4H), 7.70 (d, ^3J =4.2 Hz, 1H), 7.95 (d, ^3J =4.2 Hz, 1H), 8.1 (s, 1H), 8.13 (d, ^3J = 7.7 Hz, 1H), 8.70 (dd, ^3J =8.8 Hz, ^4J = 1.6 Hz, 1H), 8.79 (s, 1H), 9.32 (d, ^4J =1.4 Hz, 1H); ^{13}C NMR (100 MHz, $CDCl_3$): δ 14.1, 22.6, 27.0, 28.1, 29.0, 31.6, 43.3, 83.6, 100.6, 108.8, 109.2, 116.2, 118.3, 119.8, 120.9, 123.37, 123.39, 123.4, 126.2, 127.3, 128.0, 136.4, 137.3, 141.0, 142.0, 142.3, 145.2, 146.0, 149.4, 153.5, 155.6, 158.9, 161.7; ESI-MS, *m/z*: found 620.2142; calc. for $C_{35}H_{33}N_5O_2S_2$ $[M+H]^+$ 620.2148; IR, ν, cm^{-1}: 2923, 2852, 2213, 1719, 1588, 1460, 1451, 1432, 1366, 1356, 1246, 1153, 810, 746.

*tert-Butyl 2-cyano-3-(5-(4-(9-hexyl-9H-carbazol-3-yl)-[1,2,5]selenadiazolo[3,4-c]pyridin-7-yl)thiophen-2-yl)acrylate (**8g**)*

The crude product was purified by column chromatography using DCM:ethyl acetate (10:1) as the eluent to afford **8g** as a dark red solid (78%); ^{1}H NMR (300 MHz, $CDCl_3$): δ 0.84-0.91 (m, 3H), 1.26-1.35 (m, 6H), 1.61 (s, 9H), 1.89-1.91 (m, 2H), 4.32 (t, ^3J = 7.0 Hz,

2H), 7.25-7.51 (m, 4H), 7.85 (d, ^3J = 4.2 Hz, 1H), 8.03 (d, ^3J = 4.2 Hz, 1H), 8.24 (s, 1H), 8.22 (br d, ^3J = 4.0 Hz, 1H), 8.75 (dd, ^3J = 8.8 Hz, ^4J = 1.7 Hz, 1H), 8.87 (s, 1H), 9.40 (d, ^4J = 1.7 Hz, 1H); ^{13}C NMR (100 MHz, $CDCl_3$): δ 14.1, 22.6, 27.0, 28.2, 29.1, 29.8, 31.7, 43.5, 83.6, 100.6, 108.9, 109.2, 116.3, 119.9, 120.22, 120.9, 123.4, 123.5, 124.1, 126.3, 127.8, 128.7, 137.0, 137.1, 141.2, 141.7, 142.4, 145.3, 146.5, 155.2, 155.3, 159.7, 161.8; ^{77}Se NMR (75 MHz, $CDCl_3$): δ 1520.9; ESI-MS, *m/z*: found 668.1586; calc. for $C_{35}H_{33}N_5O_2SSe$ $[M+H]^+$ 668.1595; IR, ν, cm^{-1}: 2925, 2854, 2208, 1707, 1575, 1460, 1427, 1382, 1328, 1245, 1152, 1104, 807, 746.

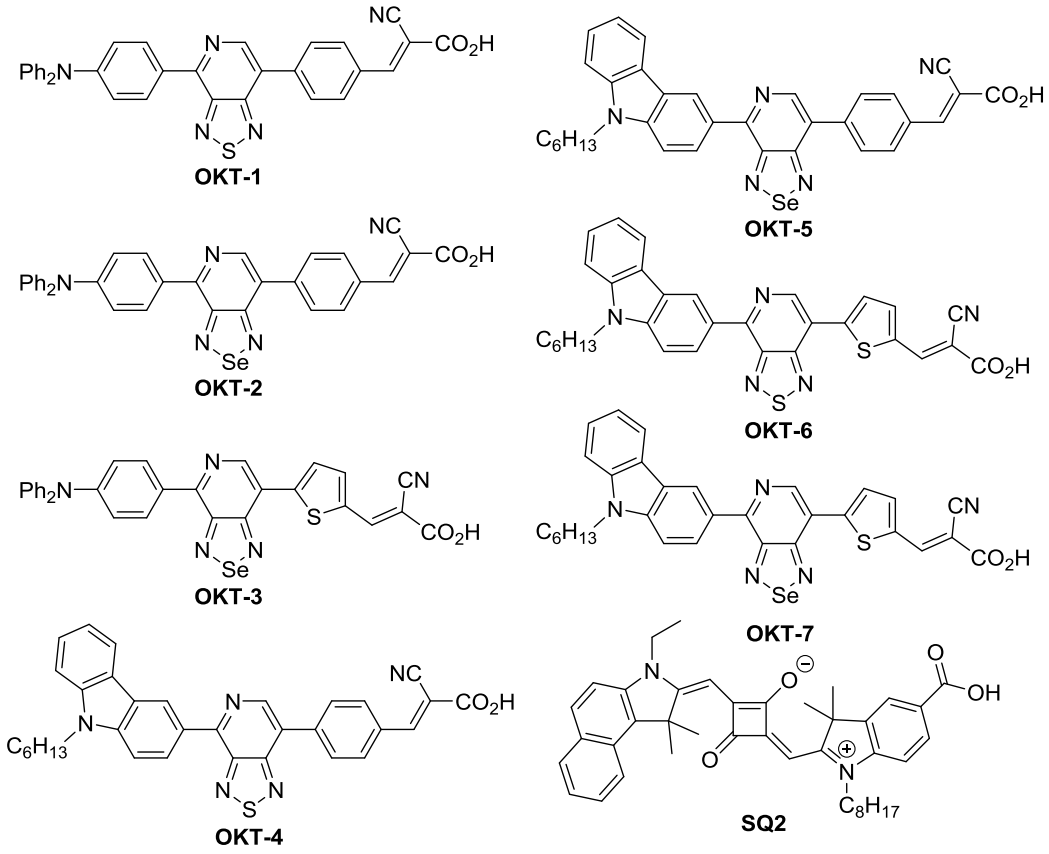

Scheme 1. Chemical structures of dyes synthesized and **SQ2**.

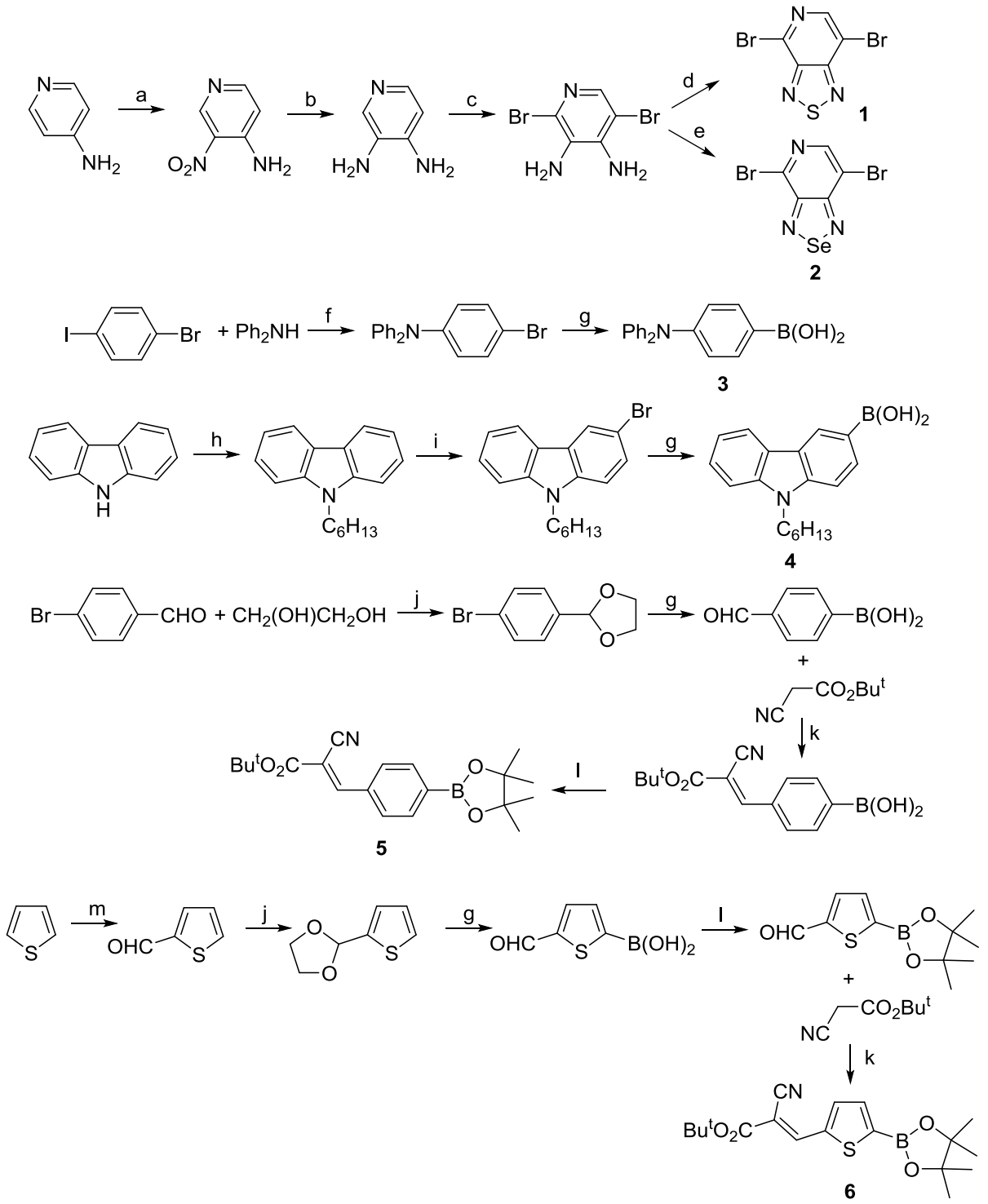

Scheme 2. Synthesis of building blocks **1-6**. The reaction conditions: (a) HNO_3/H_2SO_4; (b) H_2/Pd, EtOH; (c) Br_2, HBr; (d) $SOCl_2$, Et_3N; (e) SeO_2, EtOH; (f) 1,10-phenethroline, CuI, KOH, toluene; (g) BuLi, $B(OMe)_3$, THF; (h) $C_6H_{13}Br$, KOH, DMSO; (i) NBS, DMF, 0 °C; (j) TsOH, toluene; (k) NH_4OAc, AcOH, toluene; (l) pinacol, $MgSO_4$, THF.

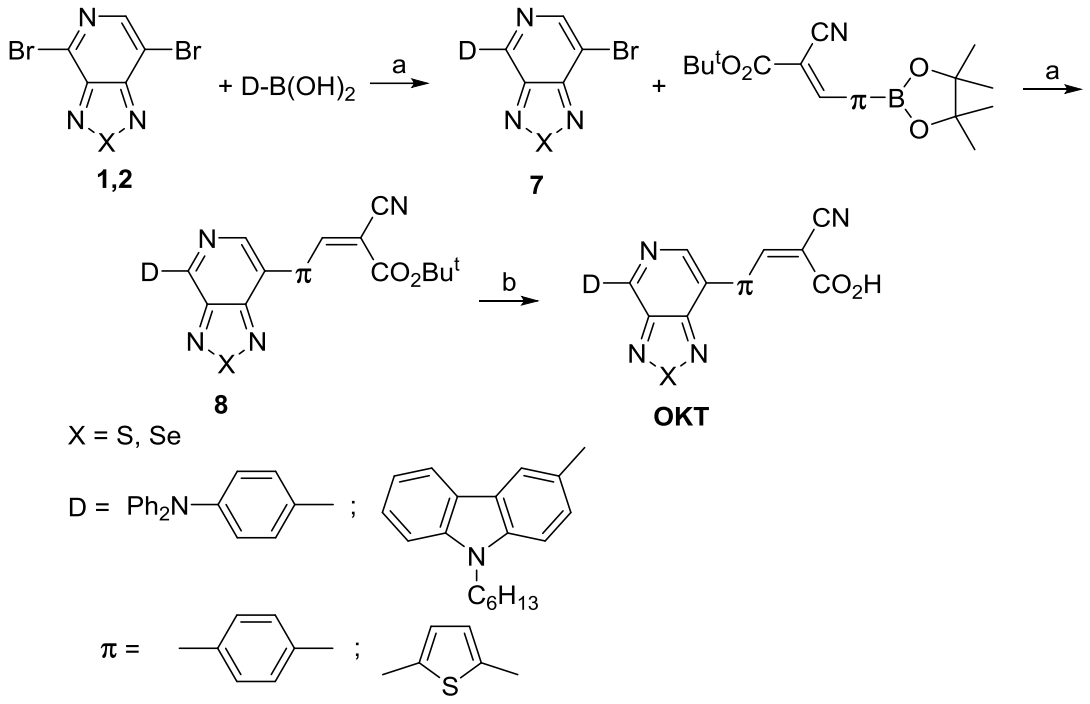

Scheme 3. Synthesis of dyes. The reaction conditions: (a) $Pd(PPh_3)_4$, K_2CO_3, THF; (b) CF_3CO_2H, CH_2Cl_2.

*2.5.4 General procedure for hydrolyses of ethers **8a-g***

To the solution of ether **8a-g** (0.3 mmol) in chloroform (10 ml) trifluoroacetic acid (6 mmol) was added and the mixture was refluxed for 4 h. after cooling the mixture was washed with water (3 × 20 ml), dried over $MgSO_4$, filtered, and concentrated under residue pressure.

2-Cyano-3-(4-(4-(4-(diphenylamino)phenyl)-[1,2,5]thiadiazolo[3,4-c]pyridin-7-yl)phenyl)acrylic acid (***OKT-1***)

The crude product was purified by column chromatography using ethanol as the eluent to afford **OKT-1** as a dark red solid (92%); IR and NMR spectra are similar to the literature data [15].

2-Cyano-3-(4-(4-(4-(diphenylamino)phenyl)-[1,2,5]selenadiazolo[3,4-c]pyridin-7-yl)phenyl)acrylic acid (***OKT-2***)

The crude product was purified by column chromatography using ethanol as the eluent to afford **OKT-2** as a violet solid (98%); ^{1}H NMR (300 MHz, DMSO-d_6): δ 7.08 (d, ^3J = 8.1 Hz, 2H), 7.14-7.20 (m, 6H), 7.37-7.42 (m, 4H), 8.20 (d, ^3J = 8.3 Hz, 2H), 8.27 (d, ^3J = 8.2 Hz, 2H), 8.42 (s, 1H), 8.53 (d, ^3J = 8.1 Hz, 2H), 8.74 (s, 1H); ^{13}C NMR (100 MHz, DMSO-d_6): δ 116.7, 120.9, 124.7, 125.7, 126.1, 130.3, 130.4, 130.5, 131.2, 131.6, 132.1, 140.1, 142.6, 146.9, 149.8, 153.5, 154.1, 154.2, 154.9, 160.2, 163.7; ^{77}Se NMR (75 MHz, DMSO-d_6): δ 1521.1; MS (MALDI-TOF), *m/z*: found 600.2 ($[M+H]^+$) calc. for $C_{33}H_{21}N_5O_2Se$

$[M+H]^+$ 600.09; IR, ν, cm^{-1}: 3435, 2930, 2232, 1684, 1588, 1452, 1331, 1212, 1146, 847, 803, 726.

2-Cyano-3-(5-(4-(4-(diphenylamino)phenyl)-[1,2,5]selenadiazolo[3,4-c]pyridin-7-yl)thiophen-2-yl)acrylic acid (***OKT-3***)

The crude product was purified by column chromatography using ethanol as the eluent to afford **OKT-3** as a violet solid (97%); ^{1}H NMR (300 MHz, DMSO-d_6): δ 7.07 (d, ^3J = 8.6 Hz, 2H), 7.17-7.20 (m, 6H), 7.39-7.44 (m, 4H), 8.12 (d, ^3J = 4.1 Hz, 1H), 8.28 (d, ^3J = 4.0 Hz, 1H), 8.55 (s, 1H), 8.57 (d, ^3J = 7.8 Hz, 2H), 9.07 (s, 1H); ^{13}C NMR (100 MHz, DMSO-d_6): δ 109.5, 116.5, 119.9, 120.3, 124.5, 125.4, 127.4, 129.7, 129.8, 131.8, 137.1, 139.7, 141.4, 146.3, 146.6, 149.6, 152.8, 154.0, 157.8, 158.2, 163.7; ^{77}Se NMR (75 MHz, DMSO-d_6): δ 1547.9; MS (MALDI-TOF), *m/z*: found 606.1569; calc. for $C_{31}H_{19}N_5O_2SSe$ $[M+H]^+$ 606.0503; IR, ν, cm^{-1}: 3430, 2925, 2855, 2218, 1679, 1584, 1331, 1205, 1145, 802, 726.

2-Cyano-3-(4-(4-(9-hexyl-9H-carbazol-3-yl)-[1,2,5]thiadiazolo[3,4-c]pyridin-7-yl)phenyl)acrylic acid (***OKT-4***)

The crude product was purified by column chromatography using ethanol as the eluent to afford **OKT-4** as a dark red solid (98%); ^{1}H NMR (300 MHz, DMSO-d_6): δ 0.81 (t, ^3J = 6.9 Hz, 3H), 1.20-1.40 (m, 6H), 1.72-1.86 (m, 2H), 4.42 (t, ^3J = 7.2 Hz, 2H), 7.24 (dd, ^3J = 8.7 Hz, ^3J =5.9 Hz, 1H), 7.48 (dd, ^3J = 7.7 Hz, ^3J =5.9 Hz, 1H), 7.61 (d,^3J = 7.7 Hz, 1H), 7.72 (d, ^3J = 8.7 Hz, 1H), 8.00 (d, ^3J = 7.5 Hz, 1H), 8.12-8.33 (m, 4H), 8.39 (s, 1H), 8.77 (d, ^3J = 8.8 Hz, 1H), 8.96 (s, 1H), 9.42 (d, ^4J = 1.4 Hz, 1H); ^{13}C NMR (100 MHz, DMSO-d_6): δ 13.8, 21.9, 26.0, 28.4, 30.8, 42.4, 103.9, 109.3, 109.7, 116.1, 119.5, 120.3, 122.32, 122.36, 122.4, 123.3, 126.2, 127.2, 127.6, 129.3, 130.8, 131.2, 138.7, 140.6, 141.4, 143.0, 148.9, 152.5, 153.4, 155.9, 163.1; MS (MALDI-TOF), *m/z*: found 558.1; calc. for $C_{33}H_{27}N_5O_2S$ $[M+H]^+$ 558.19; IR, ν, cm^{-1}: 3435, 2928, 2857, 2234, 1725, 1685, 1609, 1596, 1384, 1370, 1207,1191, 1142, 847, 803, 726.

2-Cyano-3-(4-(4-(9-hexyl-9H-carbazol-3-yl)-[1,2,5]selenadiazolo[3,4-c]pyridin-7-yl)phenyl)acrylic acid (***OKT-5***)

The crude product was purified by column chromatography using ethanol as the eluent to afford **OKT-5** as a violet solid (96%); ^{1}H NMR (300 MHz, DMSO-d_6): δ 0.79-0.84 (m, 3H), 1.04-1.09 (m, 6H), 1.76-1.89 (m, 2H), 4.46 (t, ^3J = 7.1 Hz, 2H),7.28 (dd, ^3J = 8.0 Hz, ^3J = 6.2 Hz, 1H), 7.52 (dd, ^3J = 8.2 Hz, ^3J =6.2 Hz, 1H), 7.67 (d, ^3J = 8.2 Hz, 1H), 7.76 (d, ^4J = 1.5 Hz, 1H), 7.87 (d, ^3J = 8.0 Hz, 1H), 8.11-8.05 (m, 2H), 8.16 (s, 1H), 8.20-8.27 (m, 2H), 8.75 (s, 1H), 8.78 (d, ^3J =1.4 Hz, 1H) 9.43 (d, ^4J = 1.5 Hz, 1H); ^{13}C NMR (100 MHz, DMSO-d_6):

δ 13.8, 21.9, 26.1, 28.5, 30.9, 42.5, 83.9, 109.1, 109.7, 115.7, 118.7, 119.5, 120.4, 122.1, 122.4, 122.9, 125.7, 126.1, 128.29, 129.5, 129.7, 134.7, 137.8, 140.6, 141.3 141.8, 148.0, 154.2, 157.8, 159.9, 163.8; ^{77}Se NMR (75 MHz, DMSO-d_6): δ 1542.6; MS (MALDI-TOF), *m/z*: found 606.0 ([M+H]$^+$) calc. for $C_{33}H_{27}N_5O_2Se$ [M+H]$^+$ 606.09; IR, ν, cm^{-1}: 3429, 2928, 2857, 2217, 1685, 1628, 1597, 1444, 1390, 1363, 1211, 1142, 845, 802, 726.

2-Cyano-3-(5-(4-(9-hexyl-9H-carbazol-3-yl)-[1,2,5]thiadiazolo[3,4-c]pyridin-7-yl)thiophen-2-yl)acrylic acid (***OKT-6***)

The crude product was purified by column chromatography using ethanol as the eluent to afford **OKT-6** as a dark red solid (97%); ^{1}H NMR (300 MHz, DMSO-d_6): δ 0.79-0.83 (m, 3H), 1.19-1.39 (m, 6H), 1.81-1.84 (m, 2H), 4.44 (t, ^3J = 7.0 Hz, 2H), 7.29 (dd, ^3J = 8.2 Hz, ^3J = 6.2 Hz, 1H), 7.51 (dd, ^3J = 8.8 Hz, ^3J = 6.2 Hz, 1H), 7.65 (d, ^3J = 8.2 Hz, 1H), 7.78 (d, ^3J = 8.8 Hz, 1H), 8.12 (d, ^3J = 4.2 Hz, 1H), 8.25(d, ^3J = 7.7 Hz, 1H), 8.30 (d, ^3J = 4.2 Hz, 1H), 8.53 (s, 1H), 8.83 (dd, ^3J = 8.8 Hz, ^4J = 1.6 Hz, 1H), 9.25 (s, 1H), 9.50 (d, ^4J =1.4 Hz, 1H); ^{13}C NMR (100 MHz, DMSO-d_6): δ 13.7, 21.9, 26.0, 28.4, 30.9, 42.5, 98.9, 109.4, 109.8, 115.3, 116.4, 118.2, 119.6, 120.4, 122.4, 126.3, 127.0, 127.4, 127.7, 128.6, 136.8, 139.8, 140.6, 141.6, 142.0, 145.3, 146.3, 148.7, 152.4, 154.4, 163.5; MS (MALDI-TOF), *m/z*: found 564.229; calc. for $C_{31}H_{25}N_5O_2S_2$ [M+H]$^+$ 564.1528; IR, ν, cm^{-1}: 3435, 2929, 2859, 2222, 1683, 1452, 1361, 1388, 1211, 1147, 847, 802, 726, 520.

2-Cyano-3-(5-(4-(9-hexyl-9H-carbazol-3-yl)-[1,2,5]selenadiazolo[3,4-c]pyridin-7-yl)thiophen-2-yl)acrylic acid (***OKT-7***)

The crude product was purified by column chromatography using ethanol as the eluent to afford **OKT-7** as a violet solid (93%); ^{1}H NMR (300 MHz, DMSO-d_6): δ 0.78-0.83 (m, 3H), 1.21-1.29 (m, 6H), 1.79-1.84 (m, 2H), 4.46 (t, ^3J = 6.0 Hz, 2H), 7.29 (dd, ^3J = 8.2 Hz, ^3J = 6.5 Hz, 1H), 7.51 (dd, ^3J =8.9 Hz, ^3J = 6.5 Hz, 1H), 7.67 (d, ^3J =8.2 Hz, 1H), 7.78 (d, ^3J =8.9 Hz, 1H), 8.11 (d, ^3J = 4.2 Hz, 1H), 8.23 (d, ^3J = 7.7 Hz, 1H), 8.29 (d, ^3J = 4.1 Hz, 1H), 8.53 (s, 1H), 8.77 (dd, ^3J = 8.8 Hz, ^4J= 1.9 Hz, 1H), 9.11 (s, 1H), 9.46 (d, ^4J =1.8 Hz, 1H); ^{13}C NMR (100 MHz, DMSO-d_6): δ 13.9, 22.0, 26.1, 28.5, 29.0, 31.0, 42.5, 109.4, 109.8, 116.4, 119.6, 119.8, 120.4, 122.2, 122.5, 125.3, 126.0, 126.3, 127.0, 128.0, 128.5, 137.1, 139.4, 140.7, 141.0, 141.4, 141.5, 146.2, 154.2, 158.5, 163.7; ^{77}Se NMR (75 MHz, DMSO-d_6): δ 1547.0; MS (MALDI-TOF), *m/z*: found 611.1 ([M+H]$^+$) calc. for $C_{31}H_{25}N_5O_2SSe$ [M+H]$^+$ 611.09; IR, ν, cm^{-1}: 3425, 2923, 2852, 2218, 1637, 1431, 1151, 724.

3 Results and Discussion

3.1 Synthesis and characterization

The molecular structures of the dyes are shown in Scheme 1. The general strategy for the synthesis of dyes with D-A^1-π-A^2 motif follows a stepwise approach Scheme 3. The first step was the synthesis of the internal acceptors A^1-4,7-dibromo-[1,2,5]thiadiazolo[3,4-*c*]pyridine (**1**) which was prepared by a known procedure [11] and 4,7-dibromo-[1,2,5]selenadiazolo[3,4-*c*]pyridine (**2**) which was obtained by a slightly modified method. Donor units (D) **3** and **4** were also synthesized by literature methods [12, 13]. The cross-coupling reactions of 4,7-dibromo-[1,2,5]thiadiazolo[3,4-*c*]pyridine (**1**) and 4,7-dibromo-[1,2,5]selenadiazolo[3,4-*c*]pyridine (**2**) with boronic acids **3** and **4** in the presence of $Pd(PPh_3)_4$ as a catalyst and aqua solution K_2CO_3 in THF successfully gave mono-adducts **7a-d** in high to moderate yields. The second cross-coupling of [1,2,5]selenadiazolo[3,4-*c*]pyridines **7a-d** with (4-formylphenyl)boronic acid gave bis-adducts in good yields. Unfortunately it was found that [1,2,5]selenadiazolo[3,4-*c*]pyridine moiety is unstable in the Knoevenagel condensation conditions of aldehyde derivatives with piperidine or other bases, and a different strategy was therefore required.

Mono-adducts **7a-d** were subjected to cross-coupling reaction with *tert*-butyl esters **5** and **6** in the presence of $Pd(PPh_3)_4$ as a catalyst and aqua solution K_2CO_3 in THF to afford bis-adducts **8a-g** in high yields. Final hydrolysis of compounds **8a-g** with CF_3CO_2H resulted in the formation of the target dyes in high yields. All dyes were purified by column chromatography before measurements of the physical and electrochemical properties as well as solar cell device fabrication.

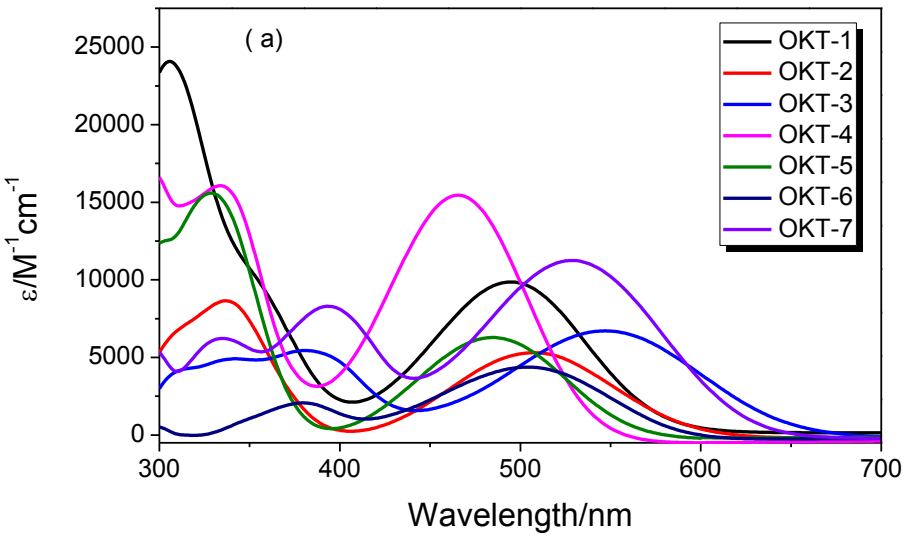

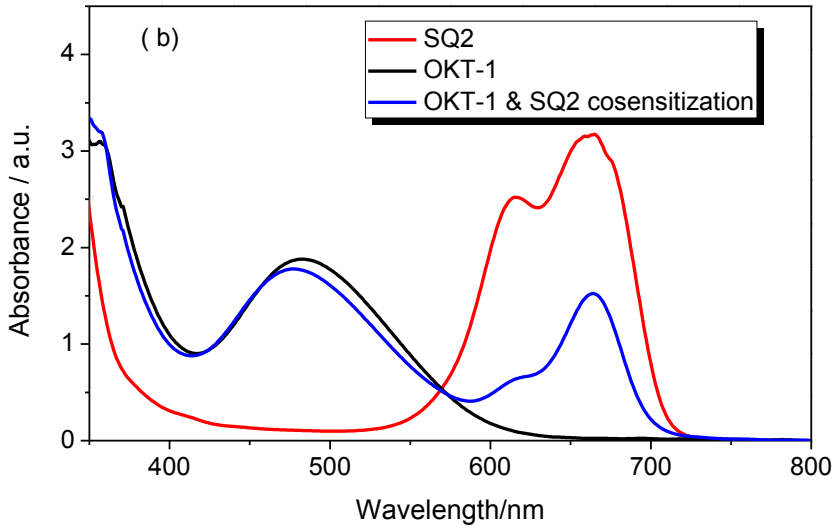

Fig. 1 UV-Visible absorption (a) in DMF/DCM (V/V=7/3) at 4×10^{-5} mol L^{-1} of **OKT** series (b) coated onto 3 μm TiO_2 film sensitized by **OKT-1**, **SQ2** and their cosensitization

3.2 Photophysical and electrochemical properties

The response region in sunlight for DSSCs is determined primarily by the UV-Vis absorption of the sensitizer. Therefore, we initially characterized the spectral response of **OKT** series in DMF/DCM (V/V=7/3) at 4×10^{-5} mol L^{-1} (Fig. 1(a)). The absorption peaks (λ_{max}) and their corresponding molar absorption coefficients (ε) are listed in Table 1. As shown in Fig. 1(a), there are two absorption regions for all the **OKT** dyes. Firstly, the absorption peaks between 300-350 nm mainly correspond to the π-π* electron transition. Secondly, the absorption bands between 450−550 nm are assigned to an intramolecular charge transfer (ICT) process between the donor and anchor/acceptor group, which produces the efficient charge-separated excited state. Due to the introduction of the thiophene ring into the conjugated spacer, **OKT-3**, **OKT-6** and **OKT-7** shown an obvious absorption about 380 nm [16]. We also observe, with Se atom replacing S in **OKT-1**, **OKT-4** and **OKT-6** to give **OKT-2**, **OKT-5** and **OKT-7**, a slight bathochromic shift of 13, 19 and 25 nm induced in the visible band in solution, respectively[17], which is conducive to the light-harvesting by the sensitizers in the photoelectric conversion process. Based on the UV-Vis results, **OKT-1**, **OKT-3**, **OKT-4** and **OKT-7** were chosen as candidates for the photovoltaic testing (Fig. 2) due to the relatively high molar absorption coefficients for all of these and the broad absorption spectra for the Se-containing **OKT-3** and **OKT-7**.

Table 1. UV-Visible absorption properties of the **OKT** series in DMF/DCM (V/V=7/3) solution.

dye	λ_{max1}/nm ($\varepsilon_{max1}\times10^3 M^{-1} cm^{-1}$)	λ_{max2}/nm ($\varepsilon_{max2}\times10^3 M^{-1} cm^{-1}$)	λ_{max3}/nm ($\varepsilon_{max3}\times10^3 M^{-1} cm^{-1}$)
OKT-1		306(22.7)	495(9.3)
OKT-2		337(9.4)	508(5.5)
OKT-3	313(7.8)	381(6.2)	547(7.9)
OKT-4		334(16.0)	466(17.3)
OKT-5		329 (17.6)	485(6.9)
OKT-6		380(3.2)	504(5.5)
OKT-7	335(7.8)	393(9.9)	529(12.7)

The electron injection and sensitizer regeneration in DSSC strongly depend on the HOMO and LUMO energy levels. And in general, their energy levels (Fig. S1 and Table 2) were roughly estimated with cyclic voltammetry (CVs) (Fig. S2) combined with UV-Vis absorption spectra (Fig. 1(a)) for the **OKT** dye series in DMF/DCM (V/V=7/3) solution [18-25]. As a result, the HOMO orbitals were -5.88, -5.84, -5.85, -6.09, -6.07, -6.09 and -6.04 eV, and the LUMO levels were -3.79, -3.98, -4.03, -3.76, -3.90, -3.97 and -4.03 eV vs. vacuum for **OKT-1-7** (Table 2), respectively. According to reference [26], the [1,2,5]selenadiazolo[3,4-*c*]pyridin ring possibly has a larger stabilization effect on the LUMO of the cyanoacrylic acid, and accordingly **OKT-2**, **OKT-5** or **OKT-7** present LUMOs with lower energy than **OKT-1**, **OKT-4** or **OKT-6**, respectively (Fig. S1). As a precondition of effective electron injection, the LUMO energy level for the studied dyes should be well above the TiO_2 conduction band (-4.0 eV). The extremely low photoelectrical conversion efficiency (PCE) for the selected dyes **OKT-3** or **OKT-7** is mainly due to their low-lying LUMO position. For a typical D-π-A dye, the HOMO level is chiefly determined by the electron donor [23], so the dyes **OKT-1-3** or **OKT-4-7** have almost same HOMO values with triphenylamine or 9-hexyl-carbazole as donors (Fig. S1), respectively. From the difference between their HOMO and the redox potential of I^-/I_3^-, there is enough regeneration driving energy for all of the **OKT** dyes.

Table 2. Electrochemical properties of the **OKT** series in DMF/DCM (V/V=7/3) solution.

Dye	E_{ox}(V) vs. NHE [a]	E_{red}(V) vs. NHE [a]	E_{gap}^{OPT} (eV) [b]	E_{gap}^{CV} (eV) [c]	E_{HOMO}(eV) vs. Vac.[d]	E_{LUMO}(eV) vs. Vac.[d]	$E_{Ex\ state}$(eV) vs. Vac.[e]
OKT-1	1.00	-1.09	2.12	2.10	-5.88	-3.79	-3.77
OKT-2	0.96	-0.90	2.01	1.86	-5.84	-3.98	-3.84
OKT-3	0.97	-0.85	1.83	1.82	-5.85	-4.03	-4.02
OKT-4	1.21	-1.12	2.23	2.33	-6.09	-3.76	-3.87
OKT-5	1.19	-0.98	2.14	2.17	-6.07	-3.90	-3.93
OKT-6	1.21	-0.91	2.07	2.12	-6.09	-3.97	-4.02
OKT-7	1.16	-0.85	1.91	2.01	-6.04	-4.03	-4.13

[a] Obtained from the oxidation (reduction) peaks; [b] E_{gap}^{OPT} (Optical gap) obtained from the absorption onset; [c] E_{gap}^{CV} (Electrochemical gap) = $E_{ox} - E_{red}$; d $E_{HOMO(LUMO)}$ = -4.88 - $E_{ox(red)}$; [e] $E_{Ex\ stat} = E_{HOMO} + E_{gap}^{OPT}$. [27]

3.3 DSC performance

3.3.1 The Photovoltaic properties of DSC devices sensitized with a single dye

According to their absorption spectra, **OKT-1**, **OKT-3**, **OKT-4** and **OKT-7** were selected to test as sensitizers in DSSCs. As presented in Fig. 2 and Table 3, the photoelectrical conversion efficiencies (PCE) of **OKT-1**, **OKT-3**, **OKT-4** and **OKT-7** were 3.10%, 0.24%, 0.56% and 0.21%, respectively. Given the modest change for fill factors (*FF*) from 0.68-0.70, the PCEs were mainly determined by the open-circuit voltage (V_{oc}) and short-circuit current density (J_{sc}). **OKT-1** shows 0.6 V V_{oc} and **OKT-3**, **OKT-4** and **OKT-7** almost have the same V_{oc} about 0.4 V. There are two main factors that result in the variation of DSSC V_{oc}. The first is the quasi-Fermi level shift and the second is recombination of injected electrons with the oxidized sensitizer or electrolyte [28]. The four dyes possess similar structures such that suppression of electronic recombination is likely to be similar in each case. Accordingly, the governing or primary factor for the voltage is more likely to be the quasi-Fermi level shift due to the different amount of injected electrons from excited dyes into conduction band of TiO_2 with various LUMO levels. For the photocurrent results, in view of the similar data of loading amount (Table 3), the different current density for **OKT-1**, **OKT-3**, **OKT-4** and **OKT-7** are mainly determined by their photophysical properties such as photoresponse region, energy levels and IPCE values. With **OKT-1**, **OKT-3**, **OKT-4** and **OKT-7** as sensitizers, the J_{sc} values were 7.39, 0.79, 1.77 and 0.71 mA cm^{-2}, respectively, which are more apparently controlled by electron injection efficiency, because relatively high J_{sc} were observed with **OKT-1** and **OKT-4** corresponding to their high LUMO position (Fig. S1). For

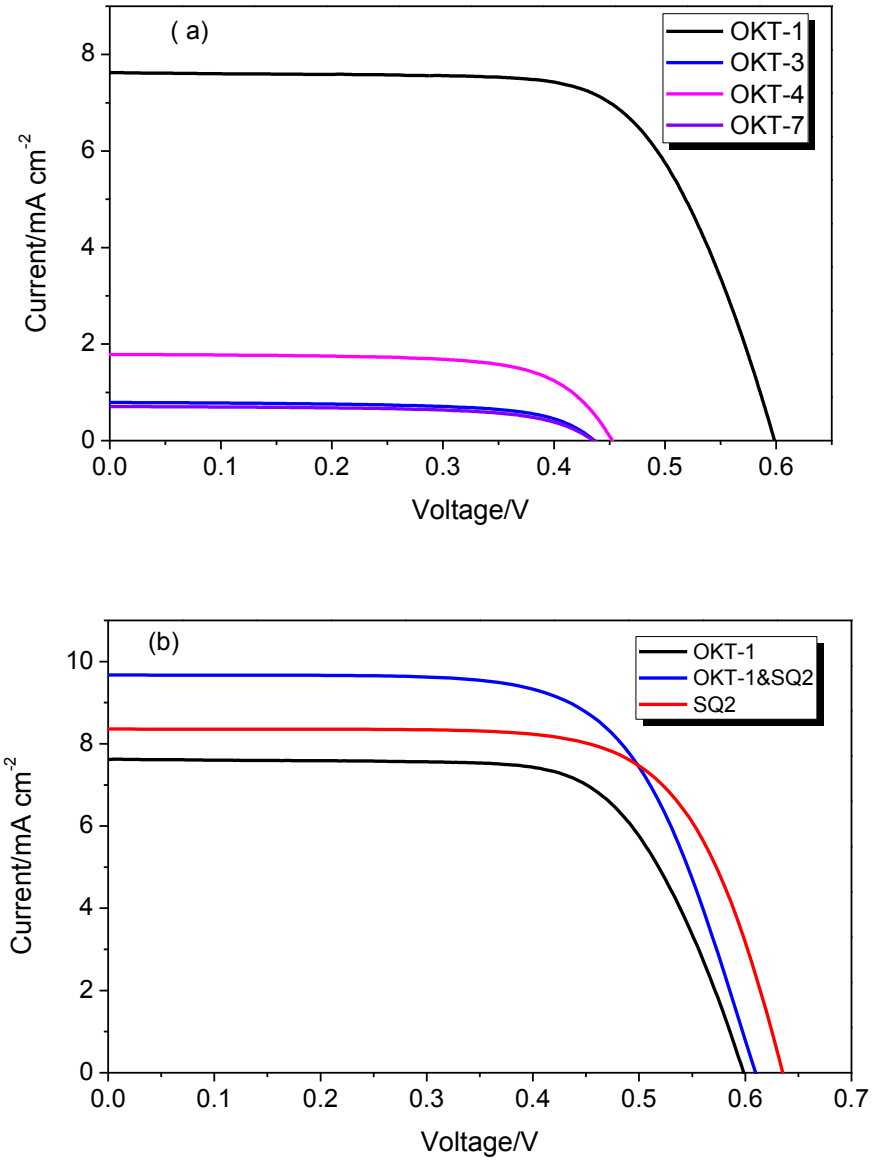

Fig. 2 Photocurrent–voltage curves of (a) **OKT-1**, **OKT-3**, **OKT-4** and **OKT-7** and (b) **OKT-1**, **SQ2** and **OKT-1** & **SQ2** sensitized TiO_2 electrodes under standard global AM 1.5 illumination (100 mW cm^{-2}).

the extremely low PCEs for **OKT-3** and **OKT-7**, the most immediate cause is the low driving force due to their LUMO levels lying close to the TiO_2 conduction band. Up to now, efficient dyes based on the carbazole donor group were realized by the connection between donor and π-spacer via the N atom [29-32]. For **OKT-1** and **OKT-4** which possess suitable energy levels, the factors limiting their PCEs may be the molar absorption coefficients and ICT process. The amount of the adsorbed dye on TiO_2 was determined by a spectroscopic method

by measuring the concentration of **OKT-1**, **OKT-3**, **OKT-4**, **OKT-7** and **SQ2** desorbed on the titania surface into a solution of 0.01 M NaOH in ethanol.

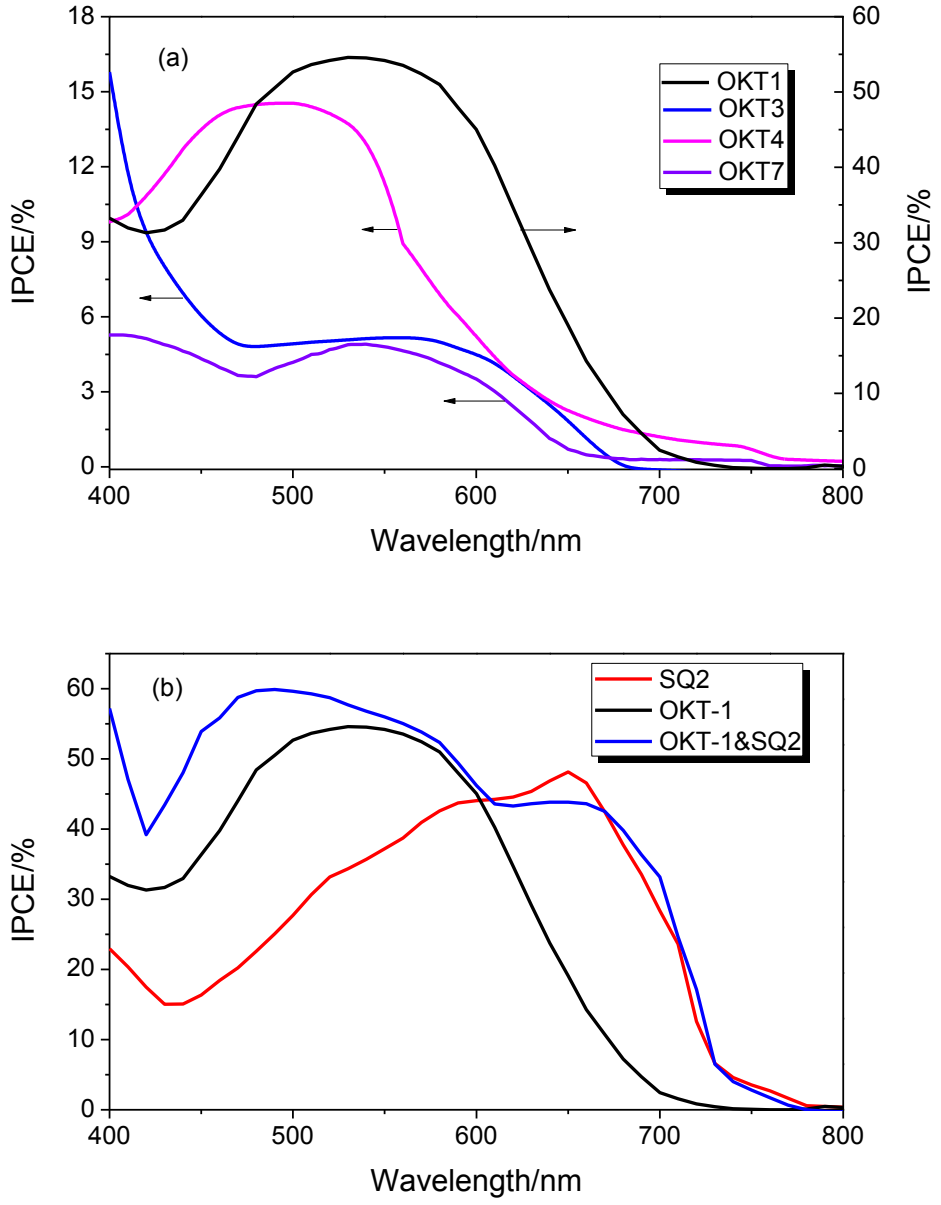

Fig. 3 IPCE of (a) **OKT-1**, **OKT-3**, **OKT-4** and **OKT-7** and (b) **OKT-1**, **SQ2** and **OKT-1** & **SQ2** sensitized TiO_2 electrodes.

The incident photon-to-electron conversion efficiency (IPCE) spectra (Fig. 3a) indicate that the visible light of different wavelengths can be converted to photocurrent efficiently in the range of 400-700 nm for **OKT-1**, **OKT-3**, **OKT-4** and **OKT-7**. Their maximum values are 54.6%, 15.8%, 14.6% and 5.27%, respectively. Notably, J_{SC} estimated from IPCE spectra are broadly comparable with those obtained from the *J*–*V* curves, and the integration of IPCE

curve for **OKT-1**, **OKT-3**, **OKT-4** and **OKT-7** are 7.15, 0.82, 1.74 and 0.69 mA cm^{-2}, respectively. Therefore, the lower photovoltaic performance for **OKT-3**, **OKT-4** and **OKT-7** can be attributed to their poor IPCE conversion with almost same V_{oc}.

*3.3.2 The improvement of PCE for **OKT-1** through cosensitization with **SQ2***

For the optimum sensitizer **OKT-1**, a significant weakness is the limited absorption at more than 600 nm. Cosensitization based on two or multiple dyes as "dye cocktails" can efficiently compensate and broaden the light-harvesting region [33]. We chose the efficient near-infrared dye **SQ2** [34, 35] as a candidate for improving the photovoltaic performance of **OKT-1** and observed a significant improvement. As shown in Fig. 1(b), a distinct absorption between 600-730 nm was observed for **OKT-1** & **SQ-2** co-sensitized TiO_2 film. The photocurrent-voltage curves of **OKT-1**, **SQ2** and **OKT-1** & **SQ2**-sensitized solar cells are depicted in Fig. 2(b) and the photovoltaic parameters are listed in Table 3. From Fig. 2(b) and Table 3, the current density of **OKT-1** was conspicuously increased with cosensitization from 7.39 mA cm^{-2} to 10.35 mA cm^{-2} and its photovoltage (0.61V) was located between those observed with the single dye **OKT-1**(0.60V) and **SQ2**(0.63V). Overall, the PCE of **OKT-1** was increased 35% from 3.10% to 4.19% when co-sensitized with **SQ2**. From Fig. 3b, with co-sensitization, the IPCE optics response was obviously enhanced from 400-600 nm and broadened from 600-750 nm as a dominant factor for the improvement of J_{sc} in co-sensitized system.

Table 3. Photovoltaic parameters for DSSCs based on **N719**, **OKT-1**, **OKT-3**, **OKT-4**, **OKT-7**, **SQ2 and OKT-1 & SQ2** (cosensitization).

Dye	V_{oc}(V)	J_{sc}(mA cm^{-2})	FF	PCE(%)	Amount/mol cm^{-2}
N719	0.74	18.31	0.69	9.36	
OKT-1	0.60	7.39	0.70	3.10	4.53×10^{-7}
OKT-3	0.44	0.79	0.68	0.24	4.21×10^{-7}
OKT-4	0.45	1.77	0.70	0.56	2.94×10^{-7}
OKT-7	0.44	0.71	0.68	0.21	4.63×10^{-7}
SQ2	0.63	8.20	0.73	3.76	2.97×10^{-7}
OKT-1 & SQ2	0.61	9.71	0.68	4.02	

4 Conclusions

In summary, we have designed and synthesized two series of D-A-π-A metal-free organic sensitizers with triphenylamine and *N*-hexyl-carbazole units as donors, respectively. Within these series, [1,2,5]selenadiazolo[3,4-*c*] pyridine and [1,2,5] thiadiazolo [3,4-*c*] pyridine were chose as auxiliary acceptors, benzene and thiophene units as π-spacer, cyanoacetate as

electron acceptor, respectively, and seven sensitizers **OKT-1-7** were prepared. It was found that the novel [1,2,5]selenadiazolo[3,4-*c*] pyridine, introduced for the first time here as an auxiliary acceptor can both broaden and red-shift the UV-Vis absorption spectrum. For this new building block to be successfully implemented however, further dye or cell design will be necessary to offset the unfavourably low LUMO energy that results. With thiophene group as π-bridge, an additional absorption peak appeared around 400nm. Finally, the structure triphenylamine + [1,2,5] thiadiazolo [3,4-c] pyridine + benzene + cyanoacetate sensitizer **OKT-1** showed the best PCE 3.10% which was increased to 4.19% when co-sensitized with squaraine-derived dye **SQ2**.

Acknowledgments

We gratefully acknowledge financial support from the Russian Science Foundation (grant no. 15-13-10022). Wenjun Wu thanks the Scientific Committee of Shanghai (14ZR1409700) for financial support. We thank the Leverhulme Trust for an International Network grant.

Supplementary data

Supplementary data associated with this article can be found, in the online version, at …

References

[1] B. Oregan, M. Grätzel, A low-cost, high-efficiency solar cell based on dye sensitized colloidal TiO_2 films, Nature 353 (1991) 737–739.

[2] A. Hagfeldt, G. Boschloo, L. Sun, L. Kloo, H. Pettersson, Dye-Sensitized Solar Cells. Chem. Rev. 110 (2010) 6595−6663.

[3] W.-Q. Wu, H.-L. Feng, H.-S. Rao, Y.-F. Xu, D.-B. Kuang, C.-Y. Su. Maximizing omnidirectional light harvesting in metal oxide hyperbranched array architectures. Nat. Commun., 5 (2014) 3968-3968.

[4] A. Mishra, M. K. R. Fischer, P. Bäuerle, Metal-Free Organic Dyes for Dye-Sensitized Solar Cells: From Structure: Property Relationships to Design Rules. Angew. Chem., Int. Ed., 48 (2009) 2474−2499.

[5] W. H. Zhu, Y. Z. Wu, S. T. Wang, W. Q. Li, X. Li, J. Chen, Z. S. Wang, H. Tian, Organic D-A-π-A Solar Cell Sensitizers with Improved Stability and Spectral Response. Adv. Funct. Mater., 21 (2011) 756−763.

[6] Y. Z. Wu, W. H. Zhu, Organic Sensitizers from D-π-A to D-A-π-A: Effect of the Internal Electron-Withdrawing Units on Molecular Absorption, Energy Levels and Photovoltaic Performances. Chem. Soc. Rev., 42 (2013) 2039−2058.

[7] Y. Z. Wu, W. H. Zhu, S. M. Zakeeruddin, M. Grätzel, Insight into D-A-π-A Structured Sensitizers: A Promising Route to Highly Efficient and Stable Dye-Sensitized Solar Cells, ACS Appl. Mater. Interfaces, 7 (2015) 9307-9318.

[8] E. A. Knyazeva, O. A. Rakitin, Influence of structural factors photovoltaic properties of dye-sensitized solar cells. Russ. Chem. Rev., 85 (2016), DOI:10.1070/RCR4649.

[9] J. Ohshita, M. Miyazaki, F.-B. Zhang, D. Tanaka, Y. Morihara, Synthesis and properties of dithienometallolepyridinochalcogenadiazole alternate polymers. Polym. J., 45 (2013) 979-984.

[10] J. Ohshita, H. Harima, Y. Morihara, A. Fujita, H. Shibuya, T. Fukumoto, π-Electron conjugated polymer having excellent thermal stability and lower band gap and org. semiconductor and organic semiconductor device using same. Jap Patent 2013237813.

[11] Y. Sun, S.-C. Chien, H.-L. Yip, Y. Zhang, K.-S. Chen, D.F. Zeigler, F.-C. Chen, B. Lin, A.K.-Y. Jen, High-mobility low-bandgap conjugated copolymers based on indacenodithiophene and thiadiazolo[3,4-c]pyridine units for thin film transistor and photovoltaic applications. J. Mater. Chem., 21(2011) 13247-13255.

[12] W. Wu, C. Cheng, W. Wu, H. Guo, S. Ji, P. Song, K. Han, J. Zhao, X. Zhang, Y. Wu, G. Du, Tuning the Emission Colour of Triphenylamine-Capped Cyclometallated Platinum(II) Complexes and Their Application in Luminescent Oxygen Sensing and Organic Light-Emitting Diodes. Eur. J. Inorg. Chem., 2010 (2010) 4683-4696.

[13] M. Tavasli, S. Bettington, M. R. Bryce, A. S. Batsanov, A. P. Monkman, Practical Syntheses of N-Hexylcarbazol-2-yl- and -3-yl-boronic Acids, Their Cross-Coupled Products and a Derived Tris-cyclometalated (Pyridin-2-yl)carbazole Iridium(III) Complex. Synthesis, 41 (2005) 1619-1624.

[14] S. Fuse, S. Sugiyama, M. M. Maitani, Y. Wada, Y. Ogomi, S. Hayase, R. Katoh, T. Kaiho, T. Takahashi, Elucidating the Structure–Property Relationships of Donor–π-Acceptor Dyes for Dye-Sensitized Solar Cells (DSSCs) through Rapid Library Synthesis by a One-Pot Procedure. Chem. Eur. J., 20 (2014) 10685-10694.

[15] S. Chaurasia, C.-Y. Hsu, H.-H. Chou, J. T. Lin, Synthesis, optical and electrochemical properties of pyridal[2,1,3]thiadiazole based organic dyes for dye sensitized solar cells. Organic Electronics, 15 (2014) 378-390.

[16] K. Hara, M. Kurashige, Y. Dan-oh, C. Kasada, A. Shinpo, S. Suga, K. Sayama, H. Arakawa, Design of new coumarin dyes having thiophene moieties for highly efficient organic-dye-sensitized solar cells, New Journal of Chemistry, 27 (2003) 783-785.

[17] D. Joly, L. Pellejà, S. Narbey, F. Oswald, T. Meyer, Y. Kervella, P. Maldivi, J.N. Clifford, E. Palomares, R. Demadrille, Metal-free organic sensitizers with narrow absorption in the visible for solar cells exceeding 10% efficiency, Energy Environ. Sci., 8 (2015) 2010-2018.

[18] W. Wu, X. Xu, H. Yang, J. Hua, X. Zhang, L. Zhang, Y. Long, H. Tian, D–π–M–π–A structured platinum acetylide sensitizer for dye-sensitized solar cells, Journal of Materials Chemistry, 21 (2011) 10666.

[19] W. Wu, J. Yang, J. Hua, J. Tang, L. Zhang, Y. Long, H. Tian, Efficient and stable dye-sensitized solar cells based on phenothiazine sensitizers with thiophene units, Journal of Materials Chemistry, 20 (2010) 1772.

[20] Z.-Y. Li, Z. Zheng, Y. Hu, Y. Wang, J. Hua, H.-B. Yang, W. Wu, Linker effect of ethylenedioxythiophenes in platinum acetylide sensitizers with hybrid starburst donors for dye-sensitized solar cells, Solar Energy, 118 (2015) 441-450.

[21] L. Yang, Z. Zheng, Y. Li, W. Wu, H. Tian, Z. Wang, N-Annulated perylene-based metal-free organic sensitizers for dye-sensitized solar cells, Chemical communications, 51 (2015) 4842-4845.

[22] X. Li, Z. Zheng, W. Jiang, W. Wu, Z. Wang, H. Tian, New D-A-pi-A organic sensitizers for efficient dye-sensitized solar cells, Chemical communications, 51 (2015) 3590-3592.

[23] W. J. Wu, J. X. Wang, Z. W. Zheng, Y. Hu, J. Y. Jin, Q. Zhang, J. L. Hua, A strategy to design novel structure photochromic sensitizers for dye-sensitized solar cells, Sci Rep, 5 (2015) 8592.

[24] Y. S. Xie, W. J. Wu, H. B. Zhu, J. C. Liu, W. W. Zhang, H. Tian, W.-H. Zhu, Unprecedentedly targeted customization of molecular energy levels with auxiliary-groups in organic solar cell sensitizers, Chem. Sci., 7 (2016) 544-549.

[25] W. J. Wu, Z. Y. Li, Z. W. Zheng, Y. Hu, J. L. Hua, π–π and p–π conjugation, which is more efficient for intermolecular charge transfer in starburst triarylamine donors of platinum acetylide sensitizers?, Dyes and Pigments, 111 (2014) 21-29.

[26] C. Climent, L. Cabau, D. Casanova, P. Wang, E. Palomares, Molecular dipole, dye structure and electron lifetime relationship in efficient dye sensitized solar cells based on donor–π–acceptor organic sensitizers, Organic Electronics, 15 (2014) 3162-3172.

[27] M. Planells, A. Abate, H.J. Snaith, N. Robertson, Oligothiophene interlayer effect on photocurrent generation for hybrid TiO_2/P3HT solar cells, ACS applied materials & interfaces, 6 (2014) 17226-17235.

[28] S. Mathew, A. Yella, P. Gao, R. Humphry-Baker, B.F. Curchod, N. Ashari-Astani, I. Tavernelli, U. Rothlisberger, M.K. Nazeeruddin, M. Gratzel, Dye-sensitized solar cells with 13% efficiency achieved through the molecular engineering of porphyrin sensitizers, Nat Chem, 6 (2014) 242-247.

[29] K. Hara, Z.-S. Wang, Y. Cui, A. Furube, N. Koumura, Long-term stability of organic–dye-sensitized solar cells based on an alkyl-functionalized carbazole dye, Energy & Environmental Science, 2 (2009) 1109.

[30] C. Chen, J.-Y. Liao, Z. Chi, B. Xu, X. Zhang, D.-B. Kuang, Y. Zhang, S. Liu, J. Xu, Metal-free organic dyes derived from triphenylethylene for dye-sensitized solar cells: tuning of the performance by phenothiazine and carbazole, Journal of Materials Chemistry, 22 (2012) 8994.

[31] J. Tang, J. L. Hua, W. J. Wu, J. Li, Z. Jin, Y. T. Long, H. Tian, New starburst sensitizer with carbazole antennas for efficient and stable dye-sensitized solar cells, Energy & Environmental Science, 3 (2010) 1736.

[32] C. Teng, X. C. Yang, C. Yuan, C. Y. Li, R. K. Chen, H. N. Tian, S. F. Li, A. Hagfeldt and L. C. Sun, Two novel carbazole dyes for dye-sensitized solar cells with open-circuit voltages up to 1 V based on Br^-/Br_3^- electrolytes, Org. Lett. , 11 (2009) 5542-5545.

[33] H. G. Tsai, C. J. Tan, W. H. Tseng, Electron Transfer of Squaraine-Derived Dyes Adsorbed on TiO2Clusters in Dye-Sensitized Solar Cells: A Density Functional Theory Investigation, The Journal of Physical Chemistry C, 119 (2015) 4431-4443.

[34] T. Maeda, N. Shima, T. Tsukamoto, S. Yagi, H. Nakazumi, Unsymmetrical squarylium dyes with π-extended heterocyclic components and their application to organic dye-sensitized solar cells, Synthetic Metals, 161 (2011) 2481-2487.

[35] B. Liu, Q. P. Chai, W. W. Zhang, W. J. Wu, H. Tian, W.-H. Zhu, Cosensitization process effect of D-A-π-A featured dyes on photovoltaic performances, Green Energy & Environment, (2016), http://dx.doi.org/10.1016/j.gee.2016.04.003.